HHS Public Access

Author manuscript

J Cardiovasc Comput Tomogr. Author manuscript; available in PMC 2025 January 01.

Published in final edited form as:

J Cardiovasc Comput Tomogr. 2024 ; 18(1): 56–61. doi:10.1016/j.jcct.2023.10.009.

Coronary artery stenosis quantification in patients with dense calcifications using ultra-high-resolution photon-counting-detector computed tomography

Emily K. Koons[a,b], **Prabhakar Shantha Rajiah, M.B.B.S., M.D.**[a], **Jamison E. Thorne**[a], **Nikkole M. Weber, R.T.(R)(CT)**[a], **Holly J. Kasten, R.T.(R)(CT)**[a], **Elisabeth R. Shanblatt, Ph.D.**[c], **Cynthia H. McCollough, Ph.D.**[a], **Shuai Leng, Ph.D.**[a,*]

[a]Department of Radiology, Mayo Clinic, 200 1st St SW, Rochester, MN, 55905. USA

[b]Department of Biomedical Engineering and Physiology, Mayo Clinic, 200 1st St SW, Rochester, MN, 55905. USA

[c]Siemens Medical Solutions, 40 Liberty Boulevard, Malvern, PA 19355. USA

Abstract

Background: To quantify differences in coronary artery stenosis severity in patients with calcified lesions between conventional energy-integrating detector (EID) CT and ultra-high-resolution (UHR) photon-counting-detector (PCD) CT.

Methods: Patients undergoing clinically indicated coronary CT angiography were prospectively recruited and scanned first on an EID-CT (SOMATOM Force, Siemens Healthineers) and then a PCD-CT (NAEOTOM Alpha, Siemens Healthineers) on the same day. EID-CT was performed with standard mode (192x0.6 mm detector collimation) following our clinical protocol. PCD-CT scans were performed under UHR mode (120x0.2mm detector collimation). For each patient, left main, left anterior descending, right coronary artery, and circumflex were reviewed and the most severe stenosis from dense calcification for each coronary was quantified using commercial software. Additionally, each measured stenosis was assigned a severity category based on percent diameter stenosis, and changes in severity category across EID-CT and PCD-CT were assessed.

Results: A total of 23 patients were enrolled, with 34 coronary artery stenoses analyzed. Stenosis was significantly reduced in PCD-CT compared to EID-CT ($p<0.001$), resulting in an average of 11% (SD=11%) reduction in percent diameter stenosis. Among the 34 lesions, 15 changed in stenosis severity category: 3 went from moderate to minimal, 1 from moderate to mild, 9 from mild to minimal, and 2 from minimal to mild with the use of PCD-CT compared to EID-CT.

[*]**Corresponding Author**: Shuai Leng, PhD, 200 First Street SW, Rochester, MN 55905, USA, Phone: (507) 284-8550, Fax: (507) 266-3661, leng.shuai@mayo.edu.

Competing Interests Statement

Elisabeth R. Shanblatt, Ph.D. is an employee of Siemens Healthineers, the manufacturer of the scanner used in this work. Cynthia H. McCollough is the recipient of a research grant to the institution from Siemens Healthineers. The remaining authors have nothing to disclose.

Conclusion: Use of UHR PCD-CT decreased percent diameter stenosis by an average of 11% relative to EID-CT, resulting in 13 of 34 stenoses being downgraded in stenosis severity category, potentially sparing patients from unnecessary intervention.

Keywords

Computed Tomography; Coronary Artery Disease; Stenosis; Photon-Counting-Detector CT; Ultra-High-Resolution

1. Introduction[1]

Cardiovascular disease is estimated to be present in 49 percent of adults over age 20,[1] with coronary artery disease (CAD) in particular being the leading cause of morbidity and mortality worldwide.[2] As the presence of coronary artery calcifications leading to vascular stenosis is an important predictor of disease severity and risk of a future cardiovascular event,[3, 4] effective assessment of stenosis severity is key to treatment. Coronary computed tomography angiography (cCTA) is now established as a first-line imaging modality, having been incorporated in multi-society guidelines for excluding significant CAD in patients presenting with stable chest pain, as well as showing high sensitivity in detection of significant coronary artery stenosis.[5] The accuracy and high negative predictive value of cCTA makes it an effective gatekeeper for invasive coronary angiography.[5]

However, a major challenge remains for the performance of cCTA in patients with dense calcifications and stents.[6–8] Calcium blooming is primarily a partial volume averaging artifact, which results in calcium appearing larger than its physical size. Blooming artifact from dense calcifications obstructs vascular lumen visualization, resulting in a decrease of diagnostic accuracy and specificity for patients with heavy calcium burden,[6, 9, 10] potentially leading to an overestimation of vascular stenosis. Since this is mainly due to the limitations of spatial resolution in conventional CT, the use of CT scanners with higher spatial resolution could potentially increase the accuracy.[11–13] Conventional CT scanners use energy-integrating-detectors (EID), which employ indirect conversion technology. Incoming x-ray photons traveling through the patient to hit the detector must be converted to optical light with a scintillator, where the light is then detected by a photodiode and converted to an electrical signal.[14, 15] This technique requires septa between pixels where no incoming photons can be detected, creating dead space, which restricts the physical ability for smaller detector pixel configurations. This limit to spatial resolution of conventional EID-CT contributes to difficulty in imaging dense calcifications.

In 2021, the first clinical photon-counting-detector (PCD) CT system was introduced commercially.[16] PCD-CT scanners employ direct conversion technology, where incoming x-ray photons are directly converted to an electrical signal via a semiconductor, skipping the intermediate scintillator step. This allows for several key advantages, including a high spatial resolution of 125 μm while maintaining dose efficiency.[17–20] With the superior spatial

[1]Abbreviations: CAD: coronary artery disease; cCTA: Coronary computed tomography angiography, EID: energy-integrating-detector; PCD: photon-counting-detector; UHR: ultra-high-resolution; ECG: electrocardiogram; VMI: virtual mono-energetic image; LM: left main; LAD: left anterior descending; RCA: right coronary artery; CX: circumflex

resolution of PCD-CT, decreases in calcium blooming artifact and improved image quality can provide a more accurate assessment of the vessel.[10, 11] In this study, we investigate the quantitative benefits of ultra-high-resolution (UHR) PCD-CT in comparison to conventional EID-CT in cCTA of patients with dense calcifications.

2. Methods

2.1 Study Population

This HIPPA compliant prospective study was approved by our institutional review board. Patients over the age of 18 suspected of having CAD who were scanned on EID-CT (SOMATOM Force, Siemens Healthineers, Forchheim, Germany) as part of their clinical care were prospectively recruited. After obtaining written informed consent, a research scan was performed on a dual-source PCD-CT (NAEOTOM Alpha, Siemens Healthineers) on the same day. Exclusion criteria for this study included the inability to provide written informed consent, pregnancy, eGFR<60, or reactions to medication administered during the clinical (EID-CT) exam.

2.2 Data Acquisition and Image Reconstruction

EID-CT scans were performed following the clinical cCTA protocol at our institution, which selects scan mode (electrocardiogram (ECG) prospectively-triggered high pitch (3.2) or sequential mode, or retrospectively gated spiral mode) based on clinical indication and patient heart rate and variability. The following EID-CT scanning parameters were used: automatic tube potential selection (CARE kV) with reference tube potential of 120 kV and slider bar at 8 (a task-specific setting optimized for soft tissue with contrast), automatic exposure control (CAREDose 4D) with quality reference effective tube-current-time product/rotation of 120 mAs; 0.25 second rotation time and 192 x 0.6 mm collimation (with z flying focal spot, physical collimation is 96 x 0.6 mm). Images were reconstructed using 0.6/0.3 mm slice thickness/increment, Bv40 kernel, 512 matrix size, and iterative reconstruction (ADMIRE) at strength 4. Study participants underwent the PCD-CT research scan immediately following their clinical EID-CT scan.

Use of cardiac beta blockers and nitroglycerin for the research scan mimicked that used clinically for the EID-CT scan. Contrast media (Omnipaque® 350, GE Healthcare, Chicago, Illinois) was administered using a weight-based injection rate: 4, 5, and 6mL/s for participants <50 kg, 50-100 kg, and >100kg, respectively. Contrast injection involves 3 phases, with injection time and contrast volume determined based on scan range (time). Once the scan range was prescribed, the scan time and post-threshold delay time were added to obtain the total injection time. The total injection time was multiplied by the weight-based injection rate (outlined above) to calculate the total injected contrast volume for the first phase. The second phase of injection was delivered with 12 mL of contrast mixed with 28 mL 0.9% NaCl (30%:70% mixture). The third phase of injection delivered 10 mL 0.9 NaCl at the same rate.

PCD-CT scans were performed using a retrospectively ECG-gated spiral acquisition mode. All PCD-CT data were acquired using an ultra-high-resolution (UHR) mode with 120 x 0.2

mm collimation and 0.25 second rotation time. Tube potential and CARE keV IQ levels were selected based on patient weight: 120 kV and 50 CARE keV IQ level for patients > 90 kg, and 90 kV and 100 CARE keV IQ level for patients <= 90 kg. CARE keV is an automatic tube potential and virtual mono-energetic image (VMI) energy level selection method on the PCD-CT scanner. However, for the UHR mode used in this study, CARE keV works similarly as that of CARE kV on the EID-CT as no multi-energy capability (e.g., VMI) is available in this mode. Therefore, tube current (IQ level) was adjusted according to the tube potential selected (50 @ 120 kV and 100 @ 90 kV). To maximize the benefits of UHR detector collimation, reconstruction with sharp kernels is necessary. However, the use of sharp kernels increases image noise, as does increased patient size. To mitigate this tradeoff of spatial resolution, image noise, and patient size, reconstruction parameters for PCD-CT were set based on patient weight to achieve the high-resolution benefits of UHR mode while keeping image noise at a reasonable level for large patients (Table 1). For each patient, image reconstruction was conducted at the cardiac phase with the least amount of motion artifact.

2.3 Stenosis Assessment

Stenosis measurement was conducted using an investigational version of a commercial software (CT Coronary Vascular Definition, syngo.via, VB70, Siemens Healthineers) as shown in Figure 1. For each patient, the most severe stenosis caused by dense calcification was identified for each segment of the left main (LM), left anterior descending (LAD), right coronary artery (RCA), and circumflex (CX). Arteries with severe motion artifact or stenosis too long along the coronary segment preventing healthy reference marker to be reliably placed were excluded from the quantification.

The software identified the coronary artery centerlines and automatically segmented the vessel lumen.[21] Once a lesion was identified, a central marker was placed over the most severe portion of the stenosis, and two markers were placed in a healthy portion of the arterial segment near the stenosis (one above and one below) to obtain the average size of the normal coronary without stenosis. The segmentation was manually reviewed, and adjustments were made if necessary. The ratio of effective diameters at the central mark and the reference markers is calculated by:

$$R = \left(\frac{D_{\text{central marker}}}{\overline{D}_{\text{reference(s)}}} \right) \tag{1}$$

where $D_{\text{central marker}}$ is the diameter of patent lumen at the central marker region with stenosis and $\overline{D}_{\text{reference(s)}}$ is the averaged diameter of two healthy portions of the arterial segment (above and below).

$$\%\,\text{Stenosis} = 100\% \times (1 - R) \tag{2}$$

Visual matching ensured that the same lesions measured for percent diameter stenosis at EID-CT were measured at PCD-CT.

2.4 Stenosis Severity Assessment

Each lesion was assigned a severity score based on the measured percentage stenosis, where a score of 0 indicated 0% or no stenosis in the segment, 1 indicated 1-24% or minimal stenosis, 2 for 25-49% or mild stenosis, 3 for 50-69% or moderate stenosis, 4 for 70-99% or severe stenosis, and 5 for 100% or total occlusion.[22] The specific values of each category were same as those used in the CAD-RADS scoring system, although in this study they were applied to individual stenosis rather than the whole patient. The stenosis category was compared between EID-CT and PCD-CT by subtracting the score of EID-CT from that of PCD-CT for each lesion. The number of lesions changing stenosis severity categories was summarized.

2.5 Statistical Analysis

Mean percent diameter stenosis for EID-CT and PCD-CT were computed and compared, with mean and standard deviation of percent diameter stenosis reduction reported. A paired two-sample *t*-test was performed to evaluate the difference of percent diameter stenosis between EID-CT and PCD-CT scans, with a p value less than 0.05 considered statistically significant. Bland-Altman analysis with 95% confidence interval limits of agreement (LOA) were conducted to assess bias in percent area stenosis comparing EID-CT to PCD-CT measurements.

3. Results

A total of 23 patients (median age 69+/−8 years old, 18 males) were enrolled in this study. Patient demographic information is summarized in Table 2. Of all patient arteries identified in this study, 33 had no calcific lesions present, 14 were excluded due to severe motion artifact, and 11 from long stenosis lesions present along the arterial segment preventing healthy reference markers to be reliably placed, resulting in a total of 34 coronary artery segments assessed for stenosis. The overall image quality was improved with the higher spatial resolution of PCD-CT. Blooming artifact was decreased compared to that of EID-CT, resulting in clearer delineation of lumen and calcification (Figure 2).

The volume CT dose index ($CTDI_{vol}$), which reports scanner output as a surrogate for patient dose, was 55+/−24 mGy for EID-CT and 36+/−12 mGy for PCD-CT. The mean percent diameter stenosis for EID-CT was 35%, which decreased to 24% with the use of UHR PCD-CT (Figure 3). PCD-CT significantly reduced the percent diameter stenosis compared to EID-CT ($p<0.001$), with an average reduction of 11% (SD = 11%). Results of Bland-Altman analysis for percent diameter stenosis between EID-CT and PCD-CT demonstrate a negative bias of 11.05, due to the fact that PCD-CT significantly decreased the percent diameter stenosis. Overall, 30 of the 34 lesions included in the study decreased in percent diameter stenosis with use of PCD-CT. Of these, 13 lesions had a decrease in stenosis grade using PCD-CT compared to EID-CT (Figure 4). Among these 13 lesions with decreased stenosis grade, 10 lesions decreased by 1 category and 3 lesions by 2 categories.

For the remaining 21 stenoses, 19 had no change, and 2 increased by 1 category with the use of PCD-CT (Table 3).

4. Discussion

This study assessed the degree of coronary artery stenosis as measured by EID-CT and PCD-CT on the same day. The use of ultra-high-resolution PCD-CT decreased coronary artery stenosis severity compared to conventional EID-CT. Based on prior *in vitro* work, the use of high spatial resolution CT imaging decreased calcium blooming artifact in the presence of dense calcifications, representing a more accurate assessment of degree of stenosis compared to a ground truth.[11, 23, 24] Koons *et al* demonstrated reduced percent area stenosis with a clinical PCD-CT compared to conventional EID-CT which overestimated the percent stenosis, more closely matching a physical reference in a phantom study of coronary artery stenosis models.[11] Sandstedt *et al* concluded that use of a prototype PCD-CT system more accurately quantified excised coronary artery calcifications in cadaveric specimens compared to EID-CT.[24] Marsh *et al* achieved similar results using a clinical PCD-CT system, showing reduced calcium blooming artifacts with PCD-CT compared to EID-CT with excised coronary artery calcification specimens compared to micro-CT as a reference standard.[23] Of the 34 lesions included in this study, 30 demonstrated a reduction in percent diameter stenosis with PCD-CT compared to EID-CT. Additionally, 13 of the 34 lesions were downgraded in stenosis severity using scores based on CAD-RADS. To the best of our knowledge, this is the first *in vivo* study comparing stenosis quantification between EID-CT and a clinical UHR PCD-CT scanner.

Small dense coronary calcifications present a challenge for CT due to blooming artifact and partial volume averaging. Therefore, the use of higher spatial resolution CT imaging for CAD has been explored.[12, 25–27] Latina *et al.* demonstrated high sensitivity and specificity of coronary stenosis measurement in severely calcified lesion using a special ultra-high-resolution EID-CT system with 0.25 mm detector pixel size (Aquilion Precision, Canon Medical System, Ōtawara, Tochigi, Japan), comparing to invasive coronary angiography (ICA) as reference.[12] In addition, PCD-CT has demonstrated notable improvements in spatial resolution compared to EID-CT and proven advantageous in coronary CTA imaging.[10, 18, 28] Recently, Hagar *et al.* conducted a prospective study for detection of CAD in a high-risk population where 68 patients were scanned with UHR PCD-CT and compared with clinical ICA for evaluation of sensitivity, specificity, and accuracy,[13] concluding that UHR PCD-CT achieved high diagnostic accuracy in CAD detection. Our study demonstrated significant reduction in percent diameter stenosis for the same patients with use of PCD-CT over conventional EID-CT, leading to potential changes in patient management directives from CAD-RADS.

Improved lumen visualization in the presence of coronary artery stenosis in patients via PCD-CT vs. EID-CT was previously evaluated using prototype PCD-CT systems. Si-Mohamed *et al.* evaluated image quality improvements using a prototype PCD-CT system with 270 μm detector pixel pitch at isocenter (SPCCT, Philips, Haifa, Israel).[28] Additionally, the benefits of using PCD-CT in overcoming blooming artifact for coronary artery stents, stenosis and plaque quantification has been shown in phantom experiments.[11, 29–31] Mergen

et al. investigated the use of a clinical PCD-CT (NAEOTOM Alpha) for cCTA imaging for CAD.[10] In this patient study, they concluded that reconstruction with kernels Bv64 and Bv72 provided superior plaque visualization.[10] Here, our study has built off these works with the use of UHR PCD-CT with 125 μm in-plane limiting spatial resolution and sharp kernel reconstruction for quantification of coronary artery stenosis as compared to conventional EID-CT in patients. Our results have demonstrated significant reduction in quantified diameter stenosis using PCD-CT, with a substantial number of cases (13/34) which decreased in stenosis severity category compared to that of EID-CT.

Our study suffers from several limitations. First, the number of patients recruited for the study was relatively small (N = 23). However, a statistically significant difference was observed in the cohort, likely due to the substantial difference between EID-CT and PCD-CT for each case. Second, our quantitative measurements lack comparison against a ground truth, e.g., from ICA. It is generally accepted that blooming artifacts overestimate the percent stenosis, which was also confirmed in previous phantom studies.[11, 29, 30] Koons *et al* showed in a phantom study that both EID-CT and PCD-CT overestimated percent stenosis compared to the ground truth, however PCD-CT estimation was closer to that of the ground truth.[11] Our results showed decrease of percent stenosis in PCD-CT compared to EID-CT. Nonetheless, future studies with a larger cohort and comparison to reference ICA are warranted. Lastly, imaging protocols, e.g., prospective vs retrospective ECG-gating, were not identically matched between EID-CT and PCD-CT. EID-CT selected prospective or retrospective gating based on patient characteristics, while retrospective gating was used in all PCD-CT acquisitions. UHR PCD-CT generates a large data set as more detector cells are used. Because of this, the current PCD-CT scanner limits the z direction collimation to 120 x 0.2 mm. There are concerns regarding the robustness of prospective gating in this narrow collimation, especially for patients with irregular heartbeats. For this reason, a more-robust retrospective gated spiral mode was used in this study. Note that the 120 x 0.2 mm collimation is a practical limitation of the data transfer, not a technical limitation of the photon counting detector technology. If faster data transfer were available in the future, wider collimation is feasible for the UHR mode and prospective gating could be used.

5. Conclusions

Our study demonstrated a decrease in percent diameter stenosis from blooming artifact reduction with the use of UHR PCD-CT compared to conventional EID-CT in a cohort of patients with dense coronary calcifications. Stenosis severity score was reduced in 13 of 34 lesions included in this study, denoting a potential change in patient management based on CAD-RADS for the individual lesions. This improved non-invasive assessment of coronary artery stenosis with dense calcifications could potentially save patients from undergoing unnecessary interventional procedures.

Acknowledgements

This work was supported in part by the National Institutes of Health under award number R01 EB028590. This content is solely the responsibility of the authors and does not necessarily represent the views of the National Institutes of Health. The authors would like to thank the CT technologists for their assistance and expertise in cardiac image reconstruction and Kevin Kimlinger for his help with manuscript preparation and submission.

Source of Funding:

Additional funding support was provided from the Department of Radiology at Mayo Clinic and the Mayo Clinic Graduate School of Biomedical Sciences.

References

1. Tsao CW, Aday AW, Almarzooq ZI, et al. Heart disease and stroke statistics—2023 update: a report from the American Heart Association. Circulation. 2023;147:e93–e621. [PubMed: 36695182]
2. Ralapanawa U, Sivakanesan R. Epidemiology and the magnitude of coronary artery disease and acute coronary syndrome: a narrative review. Journal of epidemiology and global health. 2021;11:169. [PubMed: 33605111]
3. Greenland P, Blaha MJ, Budoff MJ, Erbel R, Watson KE. Coronary calcium score and cardiovascular risk. Journal of the American College of Cardiology. 2018;72:434–447. [PubMed: 30025580]
4. Liu W, Zhang Y, Yu C-M, et al. Current understanding of coronary artery calcification. Journal of geriatric cardiology: JGC. 2015;12:668. [PubMed: 26788045]
5. Narula J, Chandrashekhar Y, Ahmadi A, et al. SCCT 2021 expert consensus document on coronary computed tomographic angiography: a report of the society of cardiovascular computed tomography. Journal of cardiovascular computed tomography. 2021;15:192–217. [PubMed: 33303384]
6. Song YB, Arbab-Zadeh A, Matheson MB, et al. Contemporary Discrepancies of Stenosis Assessment by Computed Tomography and Invasive Coronary Angiography: Analysis of the CORE320 International Study. Circulation: Cardiovascular Imaging. 2019;12:e007720. [PubMed: 30764641]
7. Dweck MR, Williams MC, Moss AJ, Newby DE, Fayad ZA. Computed tomography and cardiac magnetic resonance in ischemic heart disease. Journal of the American College of Cardiology. 2016;68:2201–2216. [PubMed: 27855810]
8. Sandstedt M, De Geer J, Henriksson L, et al. Long-term prognostic value of coronary computed tomography angiography in chest pain patients. Acta Radiologica. 2019;60:45–53. [PubMed: 29742921]
9. Kalisz K, Buethe J, Saboo SS, Abbara S, Halliburton S, Rajiah P. Artifacts at cardiac CT: physics and solutions. Radiographics. 2016;36:2064–2083. [PubMed: 27768543]
10. Mergen V, Sartoretti T, Baer-Beck M, et al. Ultra-high-resolution coronary CT angiography with photon-counting detector CT: feasibility and image characterization. Investigative Radiology. 2022;57:780–788. [PubMed: 35640019]
11. Koons E, VanMeter P, Rajendran K, Yu L, McCollough C, Leng S. Improved quantification of coronary artery luminal stenosis in the presence of heavy calcifications using photon-counting detector CT. Proceedings of SPIE--the International Society for Optical Engineering. Vol 12031: NIH Public Access; 2022.
12. Latina J, Shabani M, Kapoor K, et al. Ultra-high-resolution coronary CT angiography for assessment of patients with severe coronary artery calcification: initial experience. Radiology: Cardiothoracic Imaging. 2021;3:e210053. [PubMed: 34498007]
13. Hagar MT, Soschynski M, Saffar R, et al. Accuracy of Ultrahigh-Resolution Photon-counting CT for Detecting Coronary Artery Disease in a High-Risk Population. Radiology. 2023;307:e223305. [PubMed: 37338354]
14. Flohr T, Petersilka M, Henning A, Ulzheimer S, Ferda J, Schmidt B. Photon-counting CT review. Physica Medica. 2020;79:126–136. [PubMed: 33249223]
15. Leng S, Bruesewitz M, Tao S, et al. Photon-counting detector CT: system design and clinical applications of an emerging technology. Radiographics. 2019;39:729–743. [PubMed: 31059394]
16. FDA Clears First Major Imaging Device Advancement for Computed Tomography in Nearly a Decade. fda.gov: FDA; 2021.
17. Pourmorteza A, Symons R, Henning A, Ulzheimer S, Bluemke DA. Dose efficiency of quarter-millimeter photon-counting computed tomography: first-in-human results. Investigative radiology. 2018;53:365–372. [PubMed: 29595753]

18. Leng S, Rajendran K, Gong H, et al. 150-μm spatial resolution using photon-counting detector computed tomography technology: technical performance and first patient images. Investigative radiology. 2018;53:655–662. [PubMed: 29847412]
19. Rajendran K, Petersilka M, Henning A, et al. First clinical photon-counting detector CT system: technical evaluation. Radiology. 2022;303:130–138. [PubMed: 34904876]
20. Leng S, Yu Z, Halaweish A, et al. Dose-efficient ultrahigh-resolution scan mode using a photon counting detector computed tomography system. Journal of Medical Imaging. 2016;3:043504–043504. [PubMed: 28042589]
21. Grosskopf S, Biermann C, Deng K, Chen Y. Accurate, fast, and robust vessel contour segmentation of CTA using an adaptive self-learning edge model. Medical Imaging 2009: Image Processing. Vol 7259: SPIE; 2009:1413–1420.
22. Canan A, Kay FU, Barbosa MF, Abbara S, Rajiah PS. RadioGraphics Update: Pictorial Guide to CAD-RADS 2.0. RadioGraphics. 2023;43:e220202. [PubMed: 36995944]
23. Marsh JF Jr, VanMeter PD, Rajendran K, Leng S, McCollough CH. Ex vivo coronary calcium volume quantification using a high-spatial-resolution clinical photon-counting-detector computed tomography. Journal of Medical Imaging. 2023;10:043501–043501. [PubMed: 37408984]
24. Sandstedt M, Marsh J, Rajendran K, et al. Improved coronary calcification quantification using photon-counting-detector CT: an ex vivo study in cadaveric specimens. European radiology. 2021;31:6621–6630. [PubMed: 33713174]
25. Sarwar A, Rieber J, Mooyaart EA, et al. Calcified plaque: measurement of area at thin-section flat-panel CT and 64-section multidetector CT and comparison with histopathologic findings. Radiology. 2008;249:301–306. [PubMed: 18710960]
26. Motoyama S, Ito H, Sarai M, et al. Ultra-high-resolution computed tomography angiography for assessment of coronary artery stenosis. Circulation Journal. 2018;82:1844–1851. [PubMed: 29743388]
27. Takagi H, Tanaka R, Nagata K, et al. Diagnostic performance of coronary CT angiography with ultra-high-resolution CT: comparison with invasive coronary angiography. European journal of radiology. 2018;101:30–37. [PubMed: 29571798]
28. Si-Mohamed SA, Boccalini S, Lacombe H, et al. Coronary CT angiography with photon-counting CT: first-in-human results. Radiology. 2022;303:303–313. [PubMed: 35166583]
29. Zsarnoczay E, Fink N, Schoepf UJ, et al. Ultra-high resolution photon-counting coronary CT angiography improves coronary stenosis quantification over a wide range of heart rates–A dynamic phantom study. European Journal of Radiology. 2023;161:110746. [PubMed: 36821957]
30. Rajagopal JR, Farhadi F, Richards T, et al. Evaluation of coronary plaques and stents with conventional and photon-counting CT: benefits of high-resolution photon-counting CT. Radiology: Cardiothoracic Imaging. 2021;3:e210102. [PubMed: 34778782]
31. Koons EK, Thorne JE, Huber NR, et al. Quantifying lumen diameter in coronary artery stents with high-resolution photon counting detector CT and convolutional neural network denoising. Medical physics. 2023.

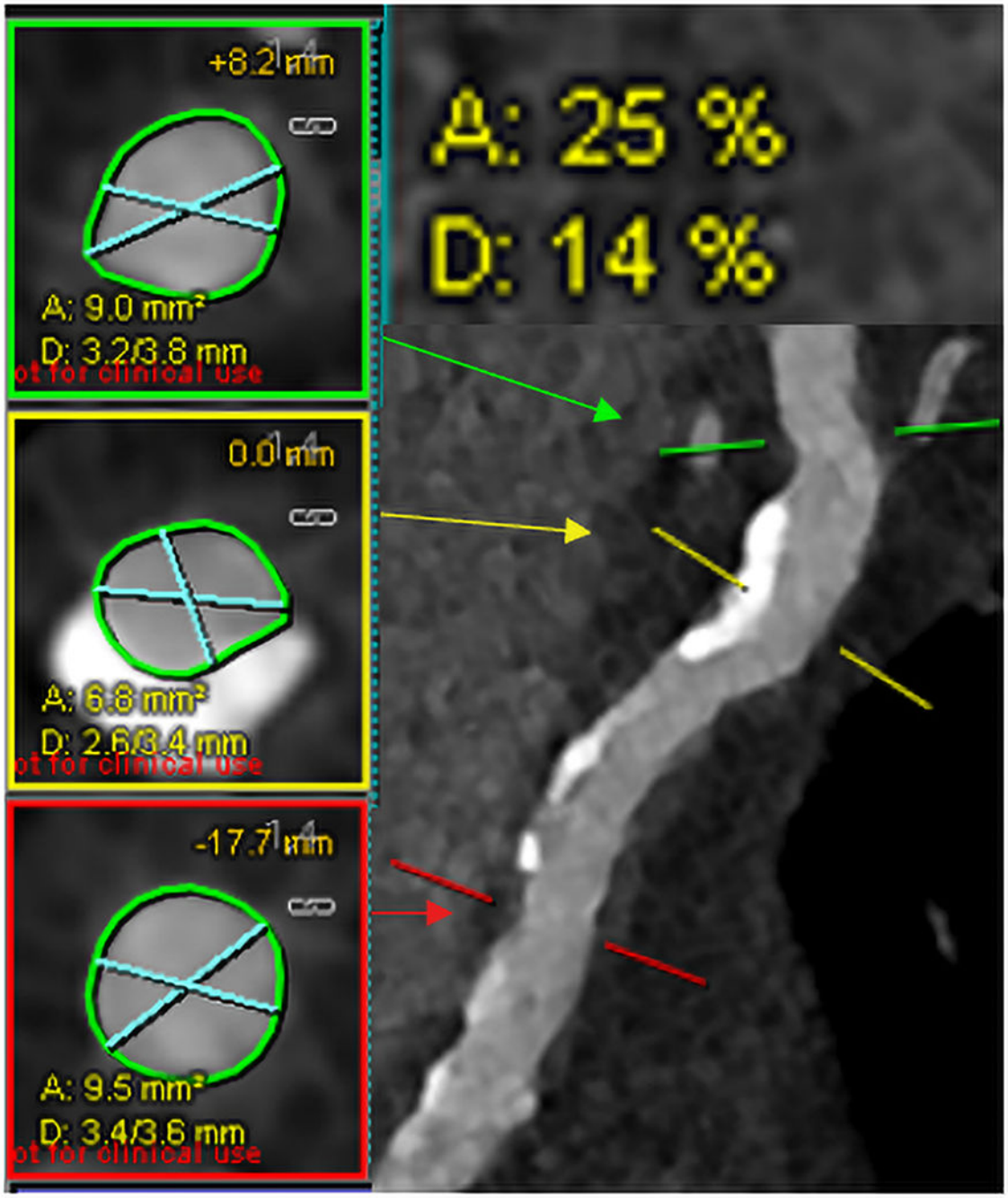

Figure 1.

Example of stenosis quantification for the proximal left anterior descending coronary artery of a representative PCD-CT case using commercial software (Syngo.via). Markers were placed at the highest stenosis (yellow, middle) and upper (green, top) and lower reference (red, bottom) locations. Respective cross-sections (left panel) with blue lines representing smallest and largest diameter were shown with percent area and diameter stenosis (upper right). (PCD=photon-counting-detector).

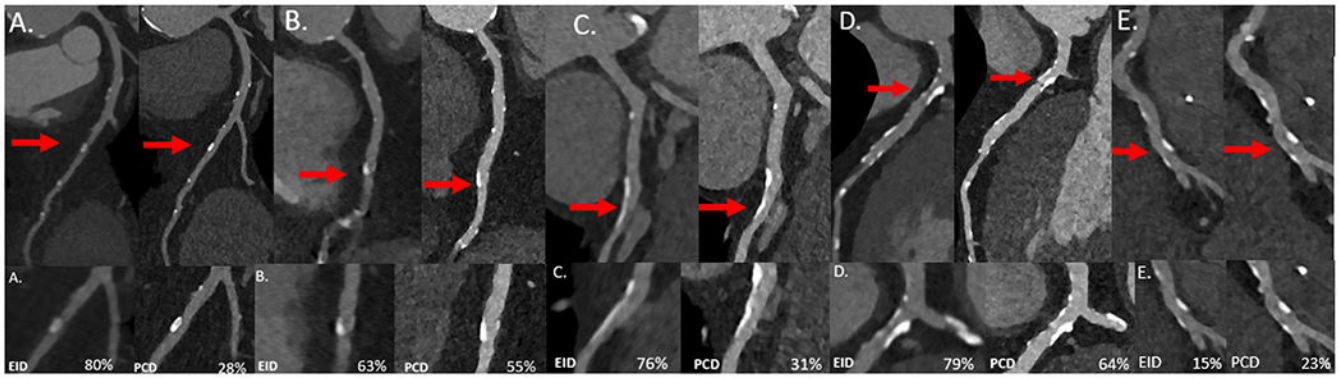

Figure 2.

Representative multiplanar reformat (MPR) patient images (EID-left; PCD-right) of the left anterior descending (LAD) (A), right coronary artery (B), LAD (C-E) with calcified plaques that were used for stenosis analysis (top). View enlarged at red arrow with percent diameter stenosis listed in bottom right for each panel (bottom).

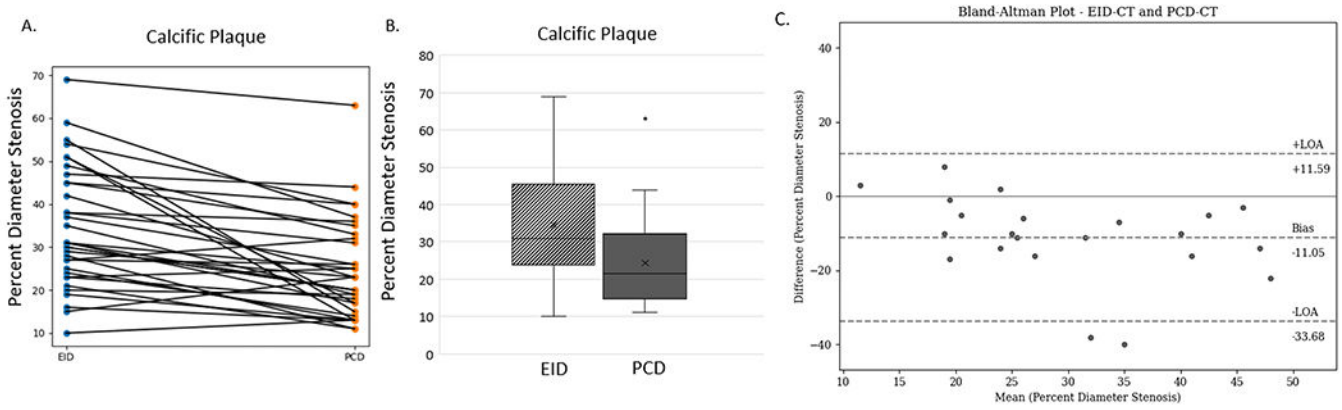

Figure 3.

(A) Results of percent diameter stenosis quantification for 34 lesions from EID (left) and PCD (right) with line connecting each individual lesion. (B) Box and whisker plot of results of percent diameter stenosis quantification for lesions measured with EID (dashed) and PCD (solid) with outliers shown. (C) Results of Bland-Altman analysis comparing EID-CT to PCD-CT for percent diameter stenosis measurements, demonstrating a negative bias of percent diameter values as PCD-CT decreased the diameter stenosis as compared to EID-CT (95% confidence interval LOA) (EID=energy-integrating-detector; PCD=photon-counting-detector, LOA = limits of agreement).

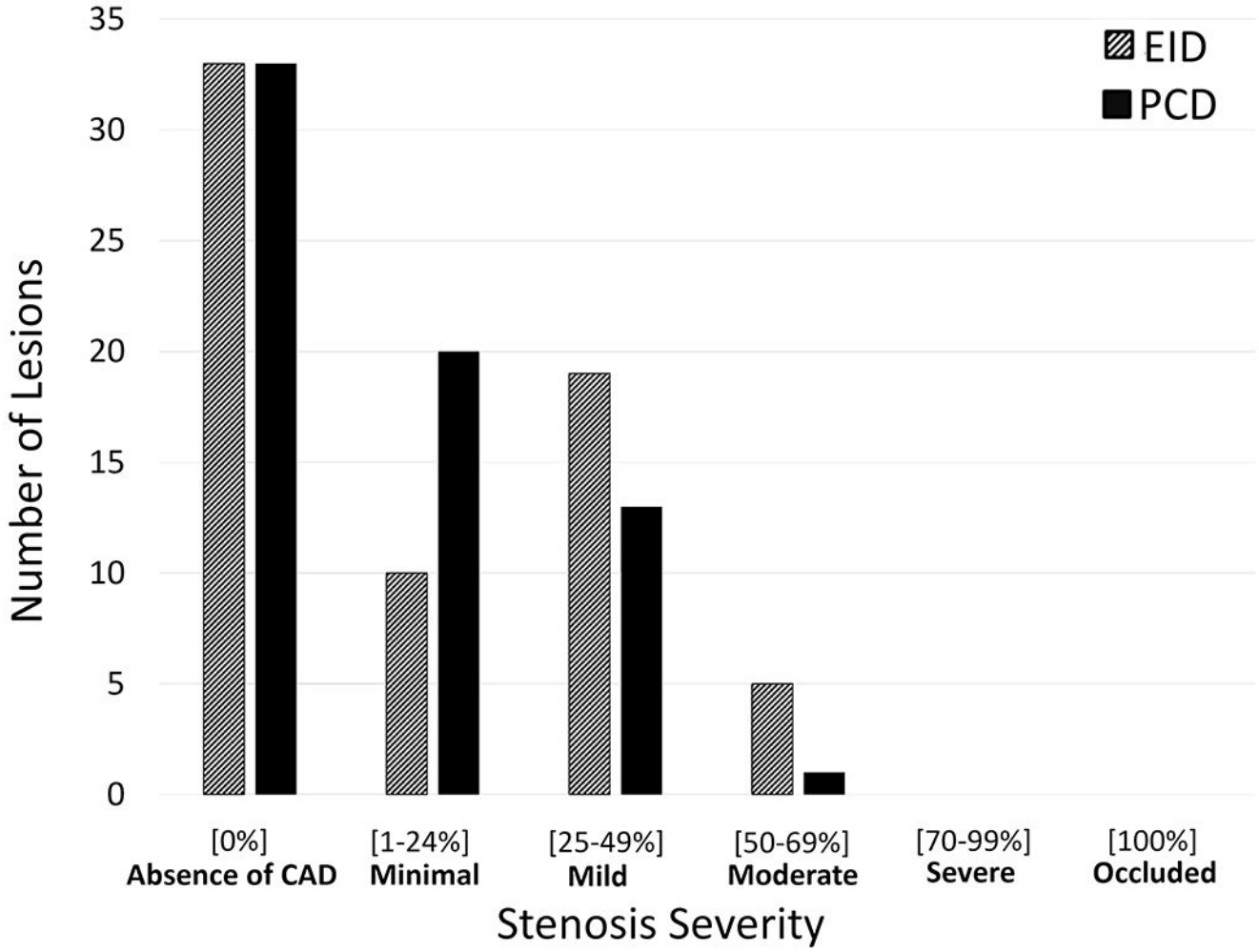

Figure 4.
Histogram of lesions and associated stenosis severity grade for EID (dashed) and PCD (solid). (EID=energy-integrating-detector; PCD=photon-counting-detector).

Table 1.

Reconstruction parameters used for photon-counting-detector-CT based on patient size.

Group	**1**	**2**	**3**
Patient weight (kg)	**<70**	**70-110**	**>110**
Reconstruction Parameters			
FOV (mm)	200	200	200
Slice Thickness (mm)	0.2	0.4	0.6
Slice Increment (mm)	0.1	0.2	0.3
Kernel	Bv64	Bv60	Bv60
QIR Strength	4	4	4
Matrix Size	1024	1024	1024

Table 2.

Patient Demographics

Characteristic	Patients
Sex assigned at birth (F)	5 (22%)
Sex assigned at birth (M)	18 (78%)
Age, y	69 +/− 8
Body mass index, kg/m^2	31 +/−5
Patients per reconstruction group based on weight	
Group 1 (<70 kg)	4
Group 2 (70-110 kg)	15
Group 3 (>110 kg)	4

Table 3.

Stenosis severity category changes from energy-integrating detector (EID-CT) to photon-counting-detector (PCD-CT).

Category Change (EID to PCD)	Shift in Stenosis Severity using PCD	# of Lesions
No Change	0	19
Moderate to Mild	−1	1
Mild to Minimal	−1	9
Moderate to Minimal	−2	3
Minimal to Mild	+1	2